Geometrical parameterization of the crystal chemistry of P63/m apatite. II. Precision, accuracy and numerical stability of the crystal-chemical Rietveld refinement

Mercier, Patrick H. J.; Le Page, Yvon; Whitfield, Pamela S.; Mitchell, Lyndon D.

Publisher's version / Version de l'éditeur:
https://doi.org/10.1107/S0021889806009903
Journal of Applied Crystallography, 39, 3, pp. 369-375, 2006-06

Journal of
Applied Crystallography
ISSN 0021-8898

Received 28 October 2005
Accepted 16 March 2006

Geometrical parameterization of the crystal chemistry of *P*63/*m* apatite. II. Precision, accuracy and numerical stability of the crystal-chemical Rietveld refinement

Patrick H. J. Mercier,[a]* Yvon Le Page,[a] Pamela S. Whitfield[a] and Lyndon D. Mitchell[b]

[a]Institute for Chemical Process and Environmental Technology (ICPET), National Research Council of Canada, Ottawa, Ontario, Canada K1A 0R6, and [b]Institute for Research in Construction (IRC), National Research Council of Canada, Ottawa, Ontario, Canada K1A 0R6. Correspondence e-mail: patrick.mercier@nrc-cnrc.gc.ca

A script developed for crystal-chemical Rietveld refinement of $P6_3/m$ apatite with *TOPAS* is implemented in parallel with standard structure refinement. Least-squares standard uncertainty (s.u.) values for directly extracted crystal-chemical parameters are nearly an order of magnitude lower than those obtained indirectly by analysis of atom coordinates derived by standard Rietveld refinement. This amazing finding originates partly in the reduction of the number of refinement parameters from 21 to 17 and partly in the fact that cell data now derive from crystal-chemical parameters instead of *vice versa*. Great precision and accuracy otherwise funneled into unit-cell parameters is then more distributed among mostly crystal-chemical distance parameters. The least-squares s.u. values are supported by analysis of numerous refinements of the same experimental data with added artificial intensity noise. Structural parameters from single-crystal results agree better with those extracted by crystal-chemical refinement. On the basis of singular value decomposition analyses performed using the program *SVDdiagnostic* [Mercier *et al.* (2006). *J. Appl. Cryst.* **39**, 458–465], crystal-chemical and standard Rietveld refinements are shown to have similar numerical stability. Crystal-chemical parameters extracted by direct Rietveld refinement, therefore, are more precise than, more accurate than and numerically as reliable as those derived from analysis of regular crystallographic refinement of the same data.

1. Introduction

Natural and synthetic apatites are conveniently described by the crystal-chemical formula $A^{\rm I}_4A^{\rm II}_6(B{\rm O}_4)_6X_2$. The $A^{\rm I}$ and $A^{\rm II}$ distinct crystallographic sites are usually occupied by larger divalent, monovalent and trivalent cations (Ca^{2+}, Pb^{2+}, Na^+, K^+, La^{3+} *etc.*), the *B* cation sites accommodate smaller metals and metalloids (P^{5+}, As^{5+}, V^{5+}, Si^{4+} *etc.*), and the *X* anion site is populated by halide (F^-, Cl^-, Br^- and I^-), hydroxy or oxide ions. The structure is tolerant to a wide range of chemical substitutions (Pan & Fleet, 2002) with charge balance attained by coupled cationic substitutions or mixing of mono- and divalent anions and vacancies in the *X* site.

Many emerging applications of apatite-type materials, such as the treatment of soils and waters contaminated by toxic metals (Chen *et al.*, 1997; Zhang & Ryan, 1999; Ioannidis & Zouboulis, 2003), the recycling of incinerator ashes with industrial or mining wastes (Eighmy *et al.*, 1998; Valsami-Jones *et al.*, 1998; Crannell *et al.*, 2000; Dong *et al.*, 2002; Dong & White, 2004*a*,*b*; Kim *et al.*, 2005), and the development of oxygen-conducting apatite-type electrolyte materials for solid oxygen fuel cells (Slater *et al.*, 2004), rely on structure refinement from Rietveld analysis of powder diffraction data for characterizing the material and the link between crystal structure and measured physical properties.

As a result of the complexity involved in the crystal chemistry, the quality of apatite crystal structure refinements has been the subject of some discussion (Felsche, 1972; McConnell, 1973; White *et al.*, 2005), and care must be taken to obtain reliable experimental crystal-structure determinations. Indeed, most Rietveld studies (*e.g.* Dong & White, 2004*a*; Kim *et al.*, 2000; Bigi *et al.*, 1989) required the use of bond constraints to obtain reasonable bond lengths for $B{\rm O}_4$ tetrahedra, *i.e.* $B{\rm O}_4$ bond lengths consistent with $B-{\rm O}$ distances computed from the tables of ionic radii given by Shannon (1976). Methods for detecting less reliable crystallographic

Table 1
Summary of the parameters refined and derived for crystal-chemical (C-CH) and standard crystallographic (CRYS) refinement models.

Table 1 in Mercier *et al.* (2005) gives all parameter definitions and symbols, as well as all equations necessary to obtain the parameters derived from those that are refined.

	C-CH	CRYS
Parameters refined	d_{AI-O1}, Δ_{AI-O}, δ_{AI}, α_{AI}, d_{B-O}, τ_{O-B-O}, ρ_{AII} or d_{AII-X}, α_{AII}, d_{AII-O3}, $\varphi_{O3-AII-O3}$ (total = 10)	a, c, AIz, $AIIx$, $AIIy$, Bx, By, O1x, O1y, O2x, O2y, O3x, O3y, O3z (total = 14)
Parameters derived	a, c, ψ_{AI-O1}, AIz, $AIIx$, $AIIy$, Bx, By, O1x, O1y, O2x, O2y, O3x, O3y, O3z	$(AI-O1)^{AIz=0}$, $\Delta_{AI-O}{}^{AIz=0}$, δ_{AI}, α_{AI}, $\langle B-O\rangle$, $\langle\tau_{O-B-O}\rangle$, ρ_{AII}, $(AII-X)$, α_{AII}, $(AII-O3)$, $\varphi_{O3-AII-O3}$, $\psi_{AI-O1}{}^{AIz=0}$

refinements have been proposed for apatites based on the geometry of the $A^{I}O_6$ coordination polyhedra (White *et al.*, 2005).

Mercier *et al.* (2005) showed that the crystallographic description of $P6_3/m$ apatite is equivalent to a geometrical parameterization based on crystal-chemical parameters representing observed polyhedral distortions (*i.e.* bond lengths, bond angles and polyhedral rotation). As the main application of the crystallographic description with least-squares cell data and fractional coordinates is to extract the crystal chemistry, this duality between crystallographic and crystal-chemical descriptions invites structure refinement directly on crystal-chemical parameters. We develop a script for such Rietveld refinements in §2 and perform them in §3. The relative precision, accuracy and numerical stability of the two types of refinements are discussed in §4, not just in terms of the regular considerations of R factor and χ^2, but also in terms of the s.u. values and conditioning of the least-squares matrix of normal equations. Our analysis relies heavily on singular value decomposition (SVD), an invaluable reformulation that could be used much more in least-squares analysis applied to structure refinement (*cf.* Watkin, 1994) and was recently used to develop a fast method for indexing powder diffraction patterns (Coelho, 2003).

2. Implementation of crystal-chemical constraints using *TOPAS*

Assuming cation-centered $A^{I}O_6$ polyhedra and BO_4 tetrahedra with uniform O—B—O bond-angle bending and four equal B—O bond lengths, Mercier *et al.* (2005) showed that the crystallographic description of $P6_3/m$ apatite (a, c and 12 atom coordinates = 14 crystallographic parameters) is equivalent to a geometrical parameterization based on the following crystal-chemical parameters and four constraints (Table 1): the A^{I}—O1 bond length, d_{AI-O1}; the difference between the A^{I}—O1 and A^{I}—O2 bond lengths, Δ_{AI-O}; the angle that the A^{I}—O1 bond makes with respect to **c**, ψ_{AI-O1}; the counter-rotation angle of the $A^{I}O_6$ polyhedra, δ_{AI}; the orientation of $A^{I}O_6$ polyhedra with respect to **a**, α_{AI}; the BO_4 bond length, d_{B-O}; the O—B—O bond-bending angle, τ_{O-B-O}; the A^{II}/A^{II} triangular side length, ρ_{AII}, or the A^{II}—X bond length, d_{AII-X}; the orientation of the $A^{II}/A^{II}/A^{II}$ triangles with respect to **a**, α_{AII}; the A^{II}—O3 bond length, d_{AII-O3}; and the O3—A^{II}—O3 bond angle, $\varphi_{O3-AII-O3}$. Three constraints concern the uniform bond-angle bending of BO_4 tetrahedra with four equal B—O bond lengths, while the fourth sets the z coordinate of the A^{I} cations to zero, so as to have cation-centered $A^{I}O_6$ polyhedra.

In this geometrical parameterization, the unit-cell parameters and fractional atomic coordinates derive from ten algebraically independent crystal-chemical parameters (d_{AI-O1}, Δ_{AI-O}, δ_{AI}, α_{AI}, d_{B-O}, τ_{O-B-O}, ρ_{AII} or d_{AII-X}, d_{AII-O3}, $\varphi_{O3-AII-O3}$, and α_{AII}; Table 1). By contrast, 14 crystallographic parameters (Table 1) are used in a structure refinement in space group $P6_3/m$ (12 atomic coordinates and two unit-cell parameters).

Equations of Mercier *et al.* (2005) deriving the cell parameters and the fractional atomic coordinates for each atom in the asymmetric unit in terms of the ten algebraically independent crystal-chemical parameters were implemented by creating an input file (*.INP) for the *TOPAS* software program (Bruker, 2005). This script (deposited as supplementary material[1]) consists of readable 'keywords' and 'macros' that offer the possibility to define and assign values to the ten crystal-chemical parameters and subsequently to optimize these parameters in a Rietveld refinement where the parameters can be fixed to specific values or restrained.

3. Experimental

3.1. Diffraction data

The powder X-ray diffraction pattern of fluorapatite, *viz.* $Ca_{10}(PO_4)_6F_2$, distributed with the programs *DBWS* (http://www.physics.gatech.edu/downloads/young/download_dbws.html) and *GSAS* (Larson & Von Dreele, 2004), was analyzed in detail.

3.2. Generation of artificial diffractograms with added random noise

To ascertain the effect that noise in diffraction intensities can have on refinement results, an arbitrary number, K, of 'artificial diffractograms' were generated from the measured diffractogram being analyzed. Let us refer to these artificial diffractograms as

$$D^{A}_{(1)}:\{2\theta_i, I^{A}_i\}, D^{A}_{(2)}:\{2\theta_i, I^{A}_i\}, \ldots, D^{A}_{(k)}:\{2\theta_i, I^{A}_i\}, \ldots, D^{A}_{(K)}:\{2\theta_i, I^{A}_i\} \quad (1)$$

and to the measured diffractogram (for a given sample) as

$$D^{M}:\{2\theta_i, I^{M}_i\}, \quad (2)$$

[1] Supplementary data for this paper are available from the IUCr electronic archives (Reference: HX5038). Services for accessing these data are described at the back of the journal.

where $\{2\theta_i, I_i^{\rm A}\}$ and $\{2\theta_i, I_i^{\rm M}\}$ denote the data sets of diffractometer angle ($2\theta_i$) and artificial ($I_i^{\rm A}$) or measured ($I_i^{\rm M}$) diffraction-intensity values for given diffractograms.

The intensities $I_i^{\rm A}$ of an artificial pattern $D_{(k)}^{\rm A}$:$\{2\theta_i, I_i^{\rm A}\}$ were obtained by adding computer-generated random noise, with two different types of uniform probability density distribution on a limited range around the measured intensities $I_i^{\rm M}$: for type-1,

$$I_i^{\rm A} = I_i^{\rm M} + (I_i^{\rm M})^{1/2}{\rm rand}[-1 < x < 1], \qquad (3a)$$

and for type-2,

$$I_i^{\rm A} = I_i^{\rm M} + [({\rm percent} \times I_i^{\rm M})/100] \times {\rm rand}[-1 < x < 1], \qquad (3b)$$

where (i) rand$[-1 < x < 1]$ is a random uniform deviate x in the range $-1 < x < 1$ with mean zero and unit variance [implemented using the routine *ran2* given by Press *et al.* (1994)] and (ii) percent is a pre-defined assumed error magnitude expressed as a percentage. Equation (3*a*) produces a uniform random noise having a 1σ standard deviation width corresponding to the 1σ error expected from measurement counting statistics. Equation (3*b*) provides a way to test the effects that different levels of uniform noise introduced in the powder diffraction intensities may have on the Rietveld refinement results. Note that the formulations of equations (3*a*) and (3*b*) ensure that no negative counts can be generated.

In this way, we constructed artificial powder diffractograms $D_{(k)}^{\rm A}$:$\{2\theta_i, I_i^{\rm A}\}$ with exactly the same number of measured points N and precisely the same values of all diffractometer angles $2\theta_i$ (where $i = 1 \ldots N$) as the original measured diffractogram $D^{\rm M}$:$\{2\theta_i, I_i^{\rm M}\}$. We then performed crystal-chemically constrained and standard Rietveld refinements on the artificial diffraction patterns $D_{(k)}^{\rm A}$:$\{2\theta_i, I_i^{\rm A}\}$ using exactly the same procedure as used for the original measured pattern $D^{\rm M}$:$\{2\theta_i, I_i^{\rm M}\}$. Each artificial pattern yielded a different data set of fitted (refined) parameters, the distributions of which were studied to analyze the errors of parameter estimation (§4.1).

4. Results and discussion

Two types of Rietveld refinement models were investigated: (i) standard Rietveld analysis based on the crystallographic description in space group $P6_3/m$ involving 14 crystallographic parameters (a, c and 12 fractional atomic coordinates; Table 1); and (ii) non-standard Rietveld analysis with in-built crystal-chemical constraints (§2) with direct least-squares refinement of ten crystal-chemical parameters (Table 1). These are referred to as 'crystallographic' and 'crystal-chemical' refinements, respectively, denoted 'CRYS' and 'C-CH' in the tables and figures.

4.1. Precision and accuracy of refined crystal-chemical parameters

The precision of least-squares refinement variables is given by the s.u. values derived from the diagonal terms of the variance/covariance matrix and printed by the least-squares program. The precision of derived quantities such as distances and angles is also quantified by their s.u. values, which are likewise derivable from the variance/covariance matrix and are printed by the distances-and-angles program. Accuracy is more difficult to assess. We derive it here through comparison with numbers obtained with single-crystal diffraction, an intrinsically better experiment with reduced intensity overlap and greater over-determination of refinement parameters.

Table 2 lists least-squares s.u. values calculated by the distances-and-angles utility in the *TOPAS* package for selected bond distances and angles. The striking feature is that the s.u. values from crystal-chemical refinement are typically several times lower than the corresponding s.u. values from standard crystallographic refinement, some of them an order of magnitude lower. Improvements in s.u. values by such ratios are hard to believe because they normally derive from, for example, counting times that are longer by two orders of magnitude rather than implementation of a simple re-parameterization scheme with few constraints as here. In order to confirm the above result, we accordingly plotted histograms of interatomic distances and angles derived from fitting 50 artificial diffractograms with both refinement methods, with the addition of three different levels of random noise, both type-1 and type-2 [equations (3*a*) and (3*b*)] (Table 3; Figs. 1 and 2). Peak heights for distributions in those histograms mostly corroborate the above least-squares s.u. ratio claim, with standard refinement displaying much broader and lower peaks than the very sharp crystal-chemical refinements. In addition, for a given parameter the centers of gravity of the crystallographic and crystal-chemical distributions differ, often by many times the s.u. of the broad crystallographic distribution, inviting the question of which is more accurate. In all cases, the crystal-chemical refinement is closer to single-crystal results for the same material (Comodi *et al.*, 2001; Saenger & Kuhs, 1992; Mackie & Young, 1973; Sudarsanan *et al.*, 1972), pointing to greater accuracy in addition to greater precision. In several cases, the refined crystal-chemical parameters actually fall within the distribution of single-crystal results. The standard Rietveld refinement by Majid & Hussain (1996) for the same material is also plotted in Figs. 1 and 2, with its strong points and weak points. Reasons for the greater precision and accuracy of the crystal-chemical refinement are discussed in §4.3, on the basis of the SVD evaluation of numerical stability for both types of refinement.

4.2. Evaluation of numerical stability using SVD

The program *SVDdiagnostic* described by Mercier *et al.* (2006) was used to assess the numerical conditioning of least-squares matrices in the two types of refinement. In that paper (see Tables 1, 2 and 3 therein), it is shown that both crystal-chemical and standard crystallographic refinements were initially poorly conditioned at best, owing to strongly correlated background and profile parameters that are in wide use for Rietveld fitting. SVD analysis indicated that it was better to fix those background and profile variables to a given set of somewhat arbitrary numerical values. Similarly, SVD analysis also indicated that occupancy factors needed to be fixed at full

Table 2
Comparison of s.u. values output by *TOPAS* for crystal-chemical (C-CH) and standard crystallographic (CRYS) refinements.

			s.u.		s.u.		s.u.		s.u.		s.u.		s.u.
C-CH													
Ca1:0	O1:4	2.39802	(42)										
	O1:0	2.39802	(42)	74.151	(16)								
	O1:3	2.39802	(42)	74.151	(16)	74.151	(16)						
	O2:1	2.44645	(63)	154.7555	(48)	123.939	(10)	93.026	(18)				
	O2:2	2.44645	(63)	75.948	(23)	93.026	(18)	154.7555	(48)	123.94	(10)		
	O2:5	2.44645	(63)	75.948	(23)	75.948	(23)	123.939	(10)	93.026	(18)	154.7555	(48)
CRYS													
Ca1:0	O1:4	2.3711	(24)										
	O1:0	2.3711	(24)	73.65	(10)								
	O1:3	2.3711	(24)	73.65	(10)	73.65	(10)						
	O2:1	2.4541	(29)	154.291	(92)	124.684	(84)	93.322	(96)				
	O2:2	2.4541	(29)	75.71	(10)	93.322	(96)	154.291	(92)	124.68	(84)		
	O2:5	2.4541	(29)	75.71	(10)	75.71	(10)	124.684	(84)	93.322	(96)	154.291	(92)
C-CH													
Ca2:0	O3:3	2.33557	(57)	102.584									
	O3:2	2.33557	(57)	141.067	(65)	102.584							
	O2:4	2.3874	(13)	85.67	(47)	85.670	(47)	152.267					
	O3:7	2.5069	(13)	74.889	(36)	77.442	(20)	135.735	(52)	81.085			
	O3:6	2.5069	(13)	59.349	(37)	74.889	(36)	135.735	(52)	77.442	(20)	81.085	
	O1:0	2.6868	(13)	149.635	(21)	149.635	(21)	100.708	(56)	72.247	(32)	72.247	(32)
CRYS													
Ca2:0	O3:2	2.3314	(20)										
	O3:3	2.3314	(20)	140.70	(13)								
	O2:4	2.3442	(29)	85.758	(61)	85.758	(61)						
	O3:7	2.5115	(25)	74.145	(81)	135.87	(11)	77.419	(53)				
	O3:6	2.5115	(25)	59.568	(93)	74.145	(81)	77.419	(53)	135.87	(11)		
	O1:0	2.6691	(25)	149.313	(55)	149.313	(55)	100.595	(94)	72.013	(74)	72.013	(74)
C-CH													
P:0	O1:0	1.53407	(50)										
	O3:1	1.53407	(37)	110.9056	(44)								
	O3:0	1.53407	(37)	108.0000	(16)	110.9056	(44)						
	O2:0	1.53407	(50)	107.9996	(39)	107.9996	(39)	110.9056	(14)				
	Ca2:4	3.0708	(14)	114.887	(33)	54.2946	(69)	54.2946	(69)	134.21	(33)		
	O2:3	3.16969	(95)	44.951	(28)	69.936	(34)	68.676	(14)	68.676	(14)	179.159	(34)
CRYS													
P:0	O3:1	1.5364	(20)										
	O3:0	1.5364	(20)	108.58	(17)								
	O1:0	1.5792	(39)	110.27	(12)	110.27	(12)						
	O2:0	1.5807	(29)	110.62	(16)	108.52	(11)	108.52	(11)				
	Ca2:4	3.0673	(11)	116.03	(14)	133.350	(86)	54.590	(86)	54.590	(86)		
	O2:3	3.115	(32)	44.558	(71)	71.47	(20)	177.908	(98)	68.69	(12)	68.69	(12)

occupancy on both refinements while refining only the isotropic displacement parameters. When freed from those correlated or redundant parameters, the conditioning of the least-squares matrices became fair, with no perceptible change in residuals, goodness-of-fit or other agreement factors. The crystal-chemical and crystallographic refinements had similar conditioning numbers, with an apparent slight advantage for standard refinement. As argued next, the latter advantage is clearly offset by the much lower s.u. values of the crystal-chemical refinement (Tables 2 and 3; Figs. 1 and 2).

4.3. Why are crystal-chemical s.u. values so much lower?

The reduction of independent geometric parameters from 14 to 10 between crystallographic and crystal-chemical refinement models (Table 1) is definitely part of the answer, but it is not the complete answer. For the final refinement scheme adopted where occupancy factors, background and certain profile variables are fixed (see Table 3 in Mercier *et al.*, 2006), the total number of refined parameters is reduced from 21 to 17 between crystallographic and crystal-chemical refinements. This means that the standard Rietveld refinement has only ~23% more parameters to refine. Therefore, it would be surprising if the nearly one order of magnitude decrease of s.u. values observed for crystal-chemical refinement (Table 2) was caused solely by a reduction in the total number of degrees of freedom between the two types of least-squares refinement, *i.e.* the *greater over-determination of refined parameters in the crystal-chemical refinement*. A quantitative determination of the extent to which the latter factor affects the calculated least-squares s.u. values was not attempted here; however, a qualitative physical argument for the lower values of crystal-chemical s.u. values can be provided as follows.

Inspection of eigenvectors for large eigenvalues in Table 3(*a*) of Mercier *et al.* (2006) shows that the variables precisely determined by standard refinement are *a*, *c* and positional parameters for the cations, which is not surprising because those parameters determine peak positions and large intensities. Together, those parameters determine none of the crystal-chemical parameters because the latter all involve O or F positions, which are all determined with poor precision in standard crystallographic refinement.

Similar inspection of Table 3(*b*) of Mercier *et al.* (2006) shows that all cation–oxygen distances are precisely determined by the least squares of crystal-chemical parameters. Together with the constraints, the precision of these values pretty much fixes the geometry of the coordination polyhedra; the remaining variables involve rigid-body motions of several O atoms each and therefore have larger effects on weak diffraction intensities than a single O-atom coordinate. Instead of wasting most of the information in the profile data on just unit-cell parameters and heavy-atom positions, crystal-chemical refinement spreads that information more evenly on interatomic distances first, and is then left with coordinated displacements of several anions that are constrained by those precise distances to be on lines or on surfaces rather than with full three-dimensional adjustability.

Finally, it should be noted that lower R_{wp} and goodness-of-fit values are obtained by crystallographic refinement. Although strictly speaking the latter observation means that

the crystal-chemical refinement solution is statistically less probable than the standard crystallographic one, we would argue that this drawback is well offset by the superior precision and accuracy of the crystal-chemical refinement method over standard Rietveld analysis. The correlation between structure and chemistry is known to be difficult for apatites (White *et al.*, 2005). As most apatite-type materials being designed for environmental applications are only available as powders (*e.g.* Kim *et al.*, 2005; Slater *et al.*, 2004), we expect the increased precision and accuracy of the refinement method

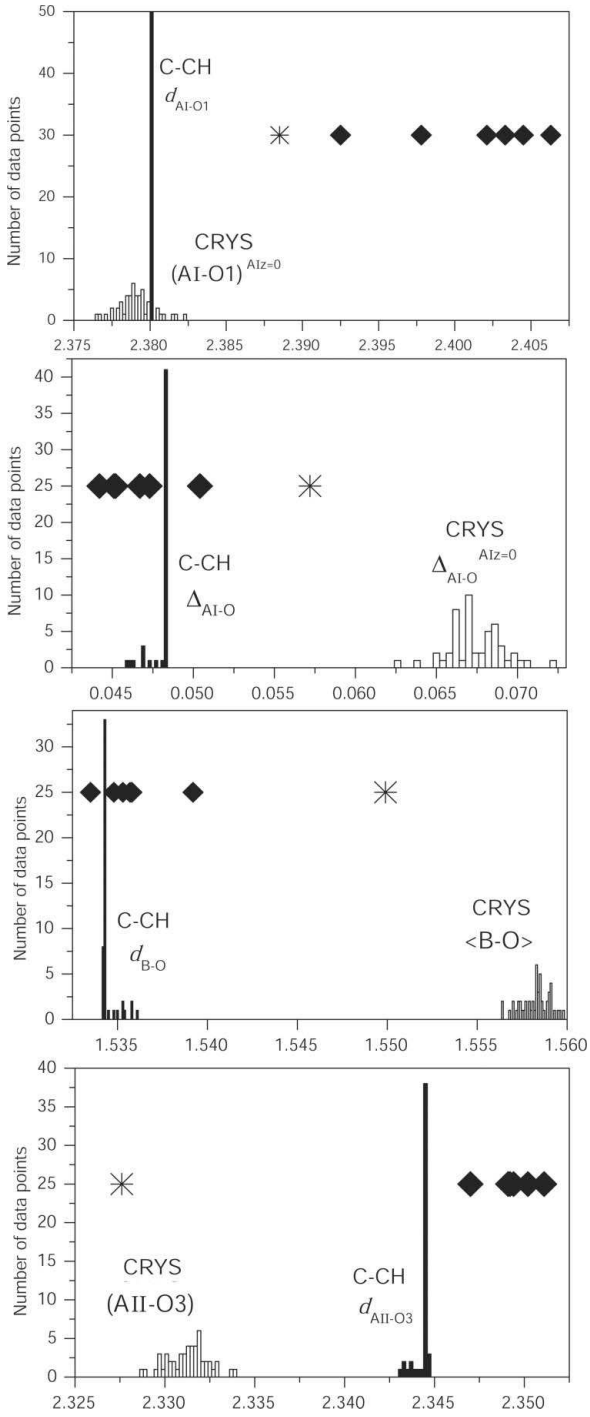

Figure 1
Comparison of bond distance parameters (Table 1) extracted by crystal-chemical (C-CH) *versus* standard crystallographic (CRYS) refinements. The distributions are derived from data sets of refined parameters for K = 50 artificial diffractograms [equation (1)] generated assuming uniform random noise of type-1 [equation (3*a*)]. Also shown are results from previously published single-crystal refinements (filled diamonds) and one Rietveld study (single stars).

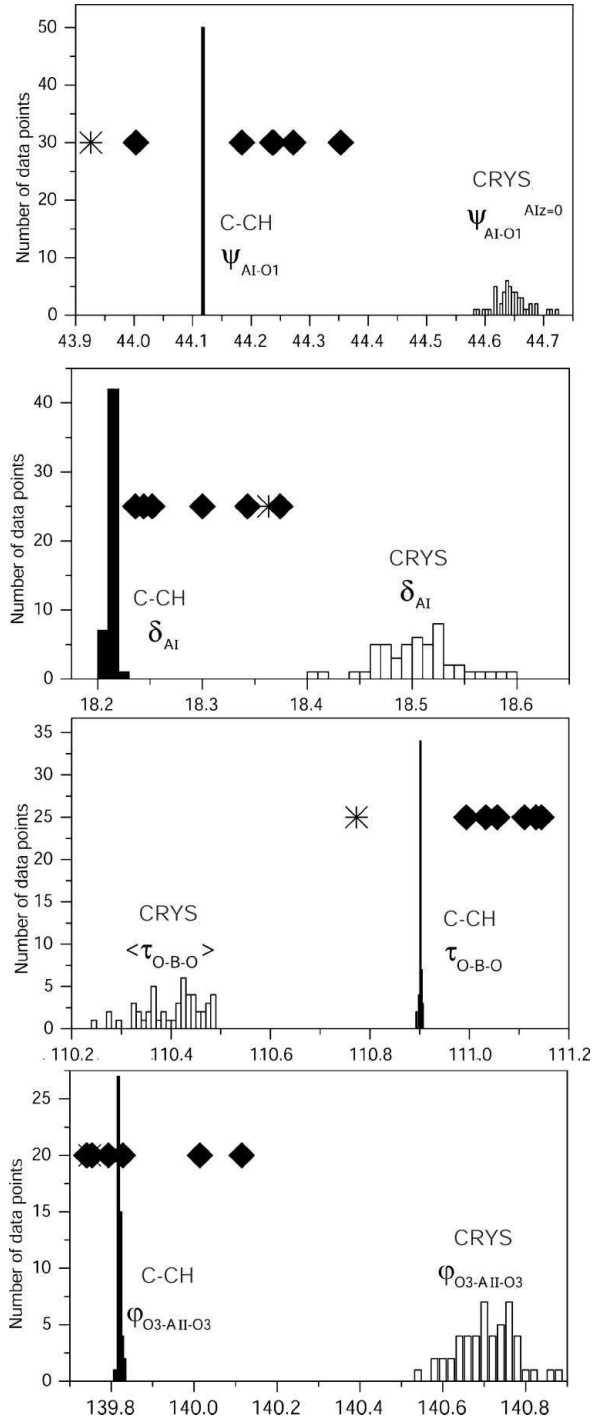

Figure 2
Comparison of bond-angle parameters (Table 1) extracted by crystal-chemical (C-CH) *versus* standard crystallographic (CRYS) refinements. The derivation of distributions and symbols is as described in the caption of Fig. 1.

Table 3
Values of mean ($\langle x \rangle$) and standard deviation (SD) for the various distributions derived from data sets of refined parameters for K = 50 artificial diffractograms [equation (1)] generated assuming either type-1 [equation (3*a*)] or type-2 [equation (3*b*)] noise.

		Type-1			Type-2 10%			Type-2 30%		
	Parameter symbols	$\langle x \rangle$	SD	100% × SD/$\lvert\langle x \rangle\rvert$	$\langle x \rangle$	SD	100% × SD/$\lvert\langle x \rangle\rvert$	$\langle x \rangle$	SD	100% × SD/$\lvert\langle x \rangle\rvert$
C-CH	a	9.37242	0.00003	0.00034	9.37245	0.00010	0.0011	9.37276	0.00174	0.01856
CRYS	a	9.37250	0.00002	0.00027	9.37252	0.00010	0.0011	9.37278	0.00065	0.00688
C-CH	c	6.88629	0.00002	0.00037	6.88631	0.000087	0.0013	6.88627	0.00203	0.029
CRYS	c	6.88634	0.00002	0.00032	6.88635	0.000087	0.0013	6.88645	0.00073	0.011
C-CH	d_{AI-O1}	2.39802	0	0	2.39802	0.000001	0.00005	2.39801	0.00004	0.0020
CRYS	$(AI-O1)_{AIz=0}$	2.3791	0.0012	0.049	2.3796	0.0040	0.16774	2.37	0.11	4.8458
C-CH	Δ_{AI-O}	0.04804	0.00062	1.3	0.04804	0.00089	1.9	0.0483	0.0022	4.6
CRYS	$\Delta_{AI-O}{}^{AIz=0}$	0.0674	0.0017	2.6	0.06677	0.00628	9.4	0.0858	0.1785	207.9
C-CH	ψ_{AI-O1}	44.117	0	0	44.1172	0.00075	0.0017	44.117	0.018	0.040
CRYS	$\psi_{AI-O1}{}^{AIz=0}$	43.645	0.029	0.067	43.6562	0.10076	0.2308	43.036	3.633	8.442
C-CH	δ_{AI}	18.2125	0.0032	0.017	18.2130	0.0057	0.031	18.22	0.11	0.61
CRYS	δ_{AI}	18.504	0.039	0.209	18.5166	0.1142	0.617	20.03	6.44	32.15
C-CH	α_{AI}	−19.780	0.0014	0.0069	−19.780	0.0033	0.017	−19.785	0.065	0.33
CRYS	α_{AI}	−21.178	0.042	0.1965	−21.212	0.1663	0.784	−20.174	4.256	21.10
C-CH	d_{B-O}	1.53441	0.00046	0.030	1.53443	0.00065	0.042	1.5346	0.0020	0.13
CRYS	$\langle B-O \rangle$	1.55819	0.00080	0.051	1.55838	0.00303	0.195	1.5889	0.0869	5.47
C-CH	τ_{O-B-O}	110.901	0.0021	0.0019	110.901	0.0035	0.0032	110.885	0.071	0.064
CRYS	$\langle \tau_{O-B-O} \rangle$	110.42	0.12	0.1080	110.401	0.1939	0.1756	110.512	4.839	4.379
C-CH	ρ_{AII}	3.99406	0.00093	0.023	3.9944	0.0032	0.081	4.05	0.24	5.92
CRYS	ρ_{AII}	3.98865	0.00173	0.043	3.9890	0.0028	0.071	4.02	0.11	2.84
C-CH	d_{AII-X}	2.30597	0.00053	0.023	2.3062	0.0019	0.081	2.339	0.138	5.9
CRYS	$(AII-X)$	2.30285	0.00100	0.043	2.3030	0.0016	0.071	2.322	0.066	2.8
C-CH	α_{AII}	118.345	0.020	0.017	118.350	0.067	0.057	117.7	2.0	1.7
CRYS	α_{AII}	118.363	0.035	0.030	118.364	0.067	0.057	118.0	1.4	1.2
C-CH	d_{AII-O3}	2.34440	0.00039	0.017	2.34438	0.00058	0.025	2.3440	0.0025	0.11
CRYS	$(AII-O3)$	2.33129	0.00114	0.049	2.33148	0.00521	0.223	2.3480	0.1723	7.34
C-CH	$\varphi_{O3-AII-O}$	139.820	0.0042	0.0030	139.821	0.0073	0.0053	139.84	0.13	0.092
CRYS	$\varphi_{O3-AII-O}$	140.707	0.0722	0.0513	140.740	0.3606	0.2562	141.90	9.77	6.888

presented here to be of considerable help in extending the knowledge base of crystal-chemical systematics for apatites.

5. Conclusions

The above analysis of the precision, accuracy and numerical stability of direct Rietveld refinement of crystal-chemical parameters of $P6_3/m$ apatite using an excellent X-ray data set shows that:

(i) The s.u. values of bond distances and angles from crystal-chemical refinement improve by nearly an order of magnitude over standard least-squares refinement of cell data and fractional coordinates. This surprising fact is corroborated by histograms from numerous refinements of the same experimental data with addition of random intensity noise, indicating much greater precision for crystal-chemical refinements.

(ii) Extracted values differ by many times their s.u. values. The much better agreement of crystal-chemical refinement results with single-crystal diffraction results indicates greater accuracy than standard Rietveld refinement.

(iii) SVD indicated that the crystal-chemical and standard crystallographic refinements had similar conditioning numbers, but the sensitivity of crystal-chemical parameters to noise in data was less if extracted directly by least squares than if calculated from refined fractional coordinates obtained by standard crystallographic refinement.

We thank Ooi Siew Ting (Nanyang Technological University, Singapore) for performing Rietveld refinements using *TOPAS* Version 3.0. We thank Alan A. Coelho and Robert B. Von Dreele for helpful hints. We also thank both anonymous referees for wise suggestions about the presentation and the substance of this study. This work was supported through the NRC/A*STAR Joint Research Programme on 'Advanced Ceramic Methods for the Co-stabilization and Recycling of Incinerator Fly Ash with Industrial Wastes'.

References

Bigi, A., Ripamonti, A., Brückner, S., Gazzano, M., Roveri, N. & Thomas, S. A. (1989). *Acta Cryst.* B**45**, 247–251.
Bruker (2005). *TOPAS*. Versions 2.1 and 3.0. Bruker AXS, Karlsruhe, Germany.
Chen, X., Wright, J. V., Conca, J. L. & Peurrung, L. M. (1997). *Water Air Soil Pollut.* **98**, 57–78.
Coelho, A. A. (2003). *J. Appl. Cryst.* **36**, 86–95.
Comodi, P., Liu, Y., Zanazzi, P. F. & Montagnoli, M. (2001). *Phys. Chem. Miner.* **28**, 219–224.
Crannell, B. S., Eighmy, T. T., Krzanowski, J. E., Eusden, J. D. Jr, Shaw, E. L. & Francis, C. A. (2000). *Waste Manage.* **20**, 135–148.
Dong, Z. & White, T. J. (2004*a*). *Acta Cryst.* B**60**, 138–145.
Dong, Z. & White, T. J. (2004*b*). *Acta Cryst.* B**60**, 146–154.
Dong, Z., White, T. J., Wei, B. & Laursen, K. (2002). *J. Am. Ceram. Soc.* **85**, 2515–2522.
Eighmy, T. T., Crannell, B. S., Krzanowski, J. E., Butler, L. G., Cartledge, F. K., Emery, E. F., Eusden, J. D. Jr, Shaw, E. L. & Francis, C. A. (1998). *Waste Manage.* **18**, 513–524.
Felsche, J. (1972). *J. Solid State Chem.* **5**, 266–275.

Ioannidis, T. A. & Zouboulis, A. I. (2003). *J. Hazard. Mater.* **B97**, 173–191.
Kim, J. Y., Dong, Z. & White, T. J. (2005). *J. Am. Ceram. Soc.* **88**, 1253–1260.
Kim, J. Y., Fenton, R. R., Hunter, B. A. & Kennedy, B. J. (2000). *Aust. J. Chem.* **53**, 679–686
Larson, A. C. & Von Dreele, R. B. (2004). *General Structure Analysis System* (*GSAS*). Report LAUR 86-748. Los Alamos National Laboratory, New Mexico, USA.
McConnell, D. (1973). *Apatite. Its Crystal Chemistry, Mineralogy, Utilization and Geologic and Biologic Occurrences*. New York: Springer.
Mackie, P. E. & Young, R. A. (1973). *J. Appl. Cryst.* **6**, 26–31.
Majid, C. A. & Hussain, M. A. (1996). *Proc. Pak. Acad. Sci.* **33**, 11–17.
Mercier, P. H. J., Le Page, Y., Whitfield, P. S. & Mitchell, L. D. (2006). *J Appl. Cryst.* **39**, 458–465.
Mercier, P. H. J., Le Page, Y., Whitfield, P. S., Mitchell, L. D., Davidson, I. J. & White, T. J. (2005). *Acta Cryst.* B**61**, 635–655.
Pan, Y. & Fleet, M. E. (2002). *Phosphates: Geochemical, Geobiological, and Materials Importance*, edited by M. J. Kohn, J. Rakovan & J. M. Hughes, pp. 13–49, *Reviews in Mineralogy and Geochemistry*, Vol. 48. Washington, DC: Mineralogical Society of America.
Press, W. H., Flannery, B. P., Teukolsky, S. A. & Vetterling, V. T. (1994). *Numerical Recipes in Fortran: The Art of Scientific Computing*, 2nd ed., reprinted with corrections. New York: Cambridge University Press.
Saenger, A. T. & Kuhs, W. F. (1992). *Z. Kristallogr.* **199**, 123–148.
Shannon, R. D. (1976). *Acta Cryst.* A**32**, 751–767.
Slater, P. R., Sansom, J. E. H. & Tolchard, J. R. (2004). *Chem. Rec.* **4**, 373–384.
Sudarsanan, K., Mackie, P. E. & Young, R. A. (1972). *Mater. Res. Bull.* **7**, 1331–1338.
Valsami-Jones, E., Ragnarsdottir, K. V., Putnis, A., Bosbach, D., Kemp, A. J. & Gressey, G. (1998). *Chem. Geol.* **151**, 215–233.
Watkin, D. (1994). *Acta Cryst.* A**50**, 411–437.
White, T. J., Ferraris, C., Kim, J. & Madhavi, S. (2005). *Apatite – An Adaptive Framework Structure*, in *Micro- and Mesoporous Mineral Phases*, edited by G. Ferraris & S. Merlino, pp. 307–373, Reviews in Mineralogy and Geochemistry, Vol. 57. Washington, DC: Mineralogical Society of America and Geochemical Society.
Zhang, P. & Ryan, J. A. (1999). *J. Environ. Sci. Technol.* **33**, 625–630.